Journal of Sound and Vibration (2001) **243**(2), 283–300
doi:10.1006/jsvi.2000.3412, available online at http://www.idealibrary.com on IDEAL®

ANALYSIS OF THE COUPLED LATERAL TORSIONAL VIBRATION OF A ROTOR–BEARING SYSTEM WITH A MISALIGNED GEAR COUPLING

M. Li

Department of Basic Courses, Xi'an University of Science and Technology, 710054, *Shaanxi, People's Republic of China. E-mail: lim@xust.sn.cn*

AND

L. Yu

Theory of Lubrication and Bearing Institute, Xi'an Jiaotong University, 710049, *Shaanxi, Peoples Republic of China*

(*Received* 15 *October* 1999, *and in final form* 10 *October* 2000)

The misalignment of a gear coupling in a multirotor system is an important problem; it can cause various faults. In the present work the non-linear coupled lateral torsional vibration model of rotor-bearing-gear coupling system is developed based on the engagement conditions of gear couplings. Theoretical analysis shows that the forces and moments acting on gear couplings due to the initial misalignment are from the inertia forces of the sleeve and the internal damping between the meshing teeth, and depend on the misalignment, internal damping, the rotating speed, and the structural parameters of the gear coupling. Numerical analysis of the signature of vibration reveals that the even-integer multiples of the rotating speed of lateral vibration and the odd-integer multiples of the torsional vibration occur in the misaligned system, and the integer multiples of vibration are apparent around the gear coupling.

1. INTRODUCTION

In rotating machinery misalignment of rotors is an important reason that leads to vibration problems. It is measured that about 60 per cent of faults was caused by misalignment. Under the misaligned condition, the vibrations can induce wear of bearings, bending deformation of shafts and so on, and threaten the stability of the system also. For a real system there are many cases to cause misalignment, for example the deformation of rotors, centers of bearings not located on the same line, errors of manufacture and installation.

Gear couplings can transmit high torque loads while accommodating misalignment between two rotors. As a part of a multirotor system, gear couplings are widely used in high-speed rotating machinery such as centrifugal compressors in large chemical processes. In the rotor system with a gear coupling misalignment is a common fault form. Dewell and Mitchell [1] considered the lateral vibration frequencies for a misaligned gear coupling; the resulting frequencies are 2, 4, 6, 8, … integer multiple components of the rotating speed, which is the judgement criterion of engineers that the coupling is under misalignment. However, the vibration of integer multiple components is not the only fault caused by the coupling misalignment, other faults such as transverse crack of a rotor and the rubbing

0022-460X/01/220283 + 18 $35.00/0

motion between rotor and stator also induce the vibration. Hence, more information on the fault diagnosis is required. In this paper, we are mainly concerned with the dynamic signature analysis of the multirotors associated with the effects of misaligned gear coupling. The excessive vibration of gear coupling in a boiler feed pump driven by a steam turbine was previously observed by Gibbons [2], who developed the misalignment forces on the coupling. However, he did not discuss the vibration signature of the system by the misalignment fault, which is very important in a fault diagnosis analysis. In the past discussions on gear coupling, the frictional forces between the teeth of couplings and its effects on the stability of the rotor systems were the mainly concern. Marmol *et al.* [3] developed a mathematical model to predict the lateral vibration of a rotor system connected with spline coupling; however, in their model some major assumptions were made, one of them was that all teeth of the coupling carry about the same load, which means that the coupling is in "perfect alignment". Nawate and Terauchi [4] analyzed the number of teeth in contact with the gear coupling considering the teeth errors; after calculating we found that there are few teeth in contact in some cases. Yamauchi and Someya [5] discussed the self-excitation vibration in the lateral direction for a crowned tooth gear coupling. Caliststit [6] measured the friction coefficients between the high-speed gear coupling teeth under several conditions. Kramer [7] discussed the bending moments on the coupling, and derived a simple equation. Bachschmid *et al.* [8] analyzed the behavior of the gear coupling between the turbine and the compressor by means of an FEM. In their dynamic model the gear coupling was simulated by a very thin beam element, so they did not consider the relative motion between the hub and the sleeve of the coupling. Kanemitsu [9] discussed the characteristics of torsional vibration about the gear coupling. Ku *et al.* [10] set up a test rig to determine the angular stiffness and equivalent viscous damping coefficients of an axial spline coupling. Regarding the vibration problems of a multirotor system connected by a coupling, Xu and Maranfoni [11] developed a theoretical model of a motor-flexible coupling-rotor system recently; the universal joint effects were included in the model to take the misalignment effects into account.

In this paper, the non-linear dynamic model for a rotor-bearing-gear coupling system is developed based on the engagement conditions of gear coupling, and the phenomena of lateral–torsional vibration of the system under the improper aligning are presented.

2. CONSTRAINT EQUATION FOR A GEAR COUPLING

Figure 1 shows an involute tooth profile and the engagement relations between the hub and the sleeve of a gear coupling. $O_i\xi_i\eta_i\zeta_i$ is the moving co-ordinate system, fixed with the sleeve. $O\xi\eta\zeta$ is the rotating co-ordinate system, ζ-axis coincides with the axis of the rotor in a static equilibrium state. The co-ordinate transformations of the two systems may be expressed as

$$\begin{aligned} \xi &= \xi_i \cos(\gamma + \theta_i) - \eta_i \sin(\gamma + \theta_i) + \xi_{ji}, \\ \eta &= \xi_i \sin(\gamma + \theta_i) + \eta_i \cos(\gamma + \theta_i) + \eta_{ji}. \end{aligned} \tag{1}$$

Let $O_e\xi_e\eta_e\zeta_e$ denote the moving co-ordinate system, fixed with the hub of the gear coupling:

$$\begin{aligned} \xi &= \xi_e \cos(\gamma + \theta_e) - \eta_e \sin(\gamma + \theta_e) + \xi_{je}, \\ \eta &= \xi_e \sin(\gamma + \theta_e) + \eta_e \cos(\gamma + \theta_e) + \eta_{je}. \end{aligned} \tag{2}$$

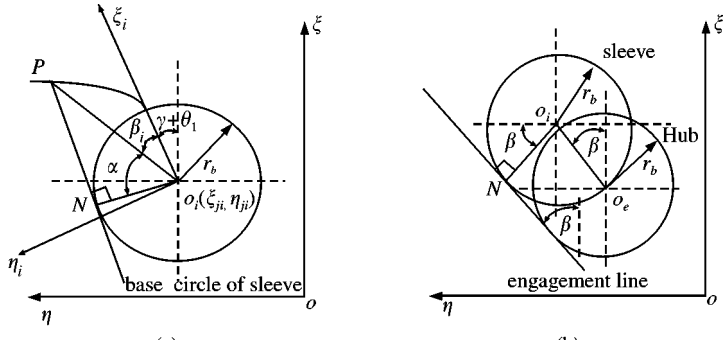

Figure 1. Engagement relations of gear coupling.

In the moving co-ordinate system, the equations of a point P on the surface of the involute tooth profile can be expressed as

$$\begin{aligned} \xi_i &= r_b(\cos\gamma_i + \gamma_i \sin\gamma_i), \\ \eta_i &= r_b(\sin\gamma_i - \gamma_i \cos\gamma_i), \end{aligned} \tag{3}$$

where $\gamma_i = \alpha + \beta_i$.

Substituting equation (3) into equation (1), it becomes

$$\begin{aligned} \xi &= r_b[\cos(\gamma_i + \theta_i + \gamma) + \gamma_i \sin(\gamma_i + \theta_i + \gamma)] + \xi_{ji}, \\ \eta &= r_b[\sin(\gamma_i + \theta_i + \gamma) - \gamma_i \cos(\gamma_i + \theta_i + \gamma)] + \eta_{ji}. \end{aligned} \tag{4}$$

In $O\xi\eta\zeta$ system the vectors of normal line and velocity of the point P are as follows:

$$n_i = \{r_b\gamma_i^3 \sin(\theta_i + \gamma_i^3 + \gamma^3) \qquad -r_b\gamma_i^3 \cos(\theta_i + \gamma_i^3 + \gamma) \qquad 0\}, \tag{5}$$

$$\mathbf{V}_p = \{\dot{\xi}_p \quad \dot{\eta}_p \quad \dot{\zeta}_p\}, \tag{6}$$

where

$$\begin{aligned} \dot{\xi}_p &= r_b[-(\dot{\theta}_i + \dot{\gamma})\sin(\theta_i + \gamma_i + \gamma) + \gamma_i \cos(\theta_i + \gamma_i + \gamma)(\dot{\gamma}_i + \dot{\theta}_i + \dot{\gamma})] + \dot{\xi}_{ji}, \\ \dot{\eta}_p &= r_b[(\dot{\theta}_i + \dot{\gamma})\cos(\theta_i + \gamma_i + \gamma) + \gamma_i \sin(\theta_i + \gamma_i + \gamma)(\dot{\gamma}_i + \dot{\theta}_i + \dot{\gamma})] + \dot{\eta}_{ji}, \\ \dot{\zeta}_p &= 0. \end{aligned}$$

The vectors of the engagement point P' on the hub tooth surface then can be also expressed as

$$\mathbf{n}_e = \{r_b\gamma_e \sin(\theta_e + \gamma_e + \gamma) \qquad -r_b\gamma_e \cos(\theta_e + \gamma_e + \gamma) \qquad 0\}, \tag{7}$$

$$\mathbf{V}_{p'} = \{\dot{\xi}_{p'} \quad \dot{\eta}_{p'} \quad \dot{\zeta}_{p'}\}, \tag{8}$$

where

$$\begin{aligned} \dot{\xi}_{p'} &= r_b[-(\dot{\theta}_e + \dot{\gamma})\sin(\theta_e + \gamma_e + \gamma) + \gamma_e \cos(\theta_e + \gamma_e + \gamma)(\dot{\gamma}_e + \dot{\theta}_e + \dot{\gamma})] + \dot{\xi}_{je}, \\ \dot{\eta}_{p'} &= r_b[(\dot{\theta}_e + \dot{\gamma})\cos(\theta_e + \gamma_e + \gamma) + \gamma_e \sin(\theta_e + \gamma_e + \gamma)(\dot{\gamma}_e + \dot{\theta}_e + \dot{\gamma})] + \dot{\eta}_{je}, \\ \dot{\zeta}_{p'} &= 0. \end{aligned}$$

Based on the conjugate engagement theorem of gear coupling, if P and P' are conjugate points, two basic conditions are necessary, which include that the normal lines of two points are parallel, and the relative velocity of two points is perpendicular to the vector of the normal lines. The latter is called engagement equation on the conjugate engagement theorem; thus, they can be expressed as

$$(1)\quad \mathbf{n}_i /\!/ \mathbf{n}_e \text{ or } \mathbf{n}_i = -\mathbf{n}_e, \qquad (2)\quad (\mathbf{V}_p - \mathbf{V}_{p'})\cdot \mathbf{n}_i = 0 \text{ or } (\mathbf{V}_p - \mathbf{V}_{p'})\cdot \mathbf{n}_e = 0. \tag{9}$$

According to the first condition $\mathbf{n}_i /\!/ \mathbf{n}_e$, from equations (5) and (7) we can obtain

$$\frac{r_b\gamma_i \sin(\theta_i + \gamma_i + \gamma)}{r_b\gamma_e \sin(\theta_e + \gamma_e + \gamma)} = \frac{-r_b\gamma_i \cos(\theta_i + \gamma_i + \gamma)}{-r_b\gamma_e \cos(\theta_e + \gamma_e + \gamma)}. \tag{10}$$

It gives

$$\theta_i + \gamma_i = \theta_e + \gamma_e. \tag{11}$$

Substituting equations (6) and (8) into the second condition $(\mathbf{V}_p - \mathbf{V}_{p'})\cdot \mathbf{n}_i = 0$, it reads as

$$(\dot{\xi}_p - \dot{\xi}_{p'})[r_b\gamma_i \sin(\theta_i + \gamma_i + \gamma)] + (\dot{\eta}_p - \dot{\eta}_{p'})[-r_b\gamma_i \cos(\theta_i + \gamma_i + \gamma)] = 0 \tag{12}$$

Using equation (11), equation (12) then becomes

$$r_b(\dot{\theta}_{ji} - \dot{\theta}_{je}) - (\dot{\xi}_{ji} - \dot{\xi}_{je})\sin(\theta_i + \gamma_i + \gamma) + (\dot{\eta}_{ji} - \dot{\eta}_{je})\cos(\theta_i + \gamma_i + \gamma) = 0. \tag{13}$$

Since the radii of base circles of the hub and the sleeve are equal, the tangent line of the two base circles (or engagement line) should be parallel to the line of centers of the base circles as shown in Figure 1, we can obtain

$$\beta + \pi/2 = \theta_i + \gamma_i + \gamma = \theta_i + \beta_i + \alpha + \gamma. \tag{14}$$

Thus,

$$\begin{aligned} \sin(\theta_i + \gamma_i + \gamma) &= \cos\beta = (\xi_{ji} - \xi_{je})/\sqrt{(\xi_{ji} - \xi_{je})^2 + (\eta_{ji} - \eta_{je})^2}, \\ \cos(\theta_i + \gamma_i + \gamma) &= -\sin\beta = -(\eta_{ji} - \eta_{je})/\sqrt{(\xi_{ji} - \xi_{je})^2 + (\eta_{ji} - \eta_{je})^2}, \end{aligned} \tag{15}$$

where β is the angle between the line of centers and ξ direction. Substituting equation (15) into equation (13), it can be expressed as

$$r_b(\dot{\theta}_{ji} - \dot{\theta}_{je}) = \frac{(\xi_{ji} - \xi_{je})}{\sqrt{(\xi_{ji} - \xi_{je})^2 + (\eta_{ji} - \eta_{je})^2}}(\dot{\xi}_{ji} - \dot{\xi}_{je}) + \frac{(\eta_{ji} - \eta_{je})}{\sqrt{(\xi_{ji} - \xi_{je})^2 + (\eta_{ji} - \eta_{je})^2}}(\dot{\eta}_{ji} - \dot{\eta}_{je}). \tag{17}$$

Integrating the above equation, finally we can obtain

$$r_b^2(\theta_{ji} - \theta_{je})^2 = (\xi_{ji} - \xi_{je})^2 + (\eta_{ji} - \eta_{je})^2. \tag{18}$$

Equation (18) is a constraint condition that should be satisfied in normal meshing between the lateral displacements in the centers and torsional angles of the hub and the sleeve of gear couplings, and the constraint is holonomic on analytical mechanics.

3. MODELLING OF THE GEAR COUPLING HALVES

Figure 2(a) shows a rotor-gear coupling system that may be separated by n-station, n-section breakup. There are five d.o.f. per station ($\xi, \eta, \delta, \varepsilon, \theta$ shown in Figure 2(b), neglecting the displacement in the z direction). $Oxyz$ is the fixed co-ordinate system, where x- and y-axis are vertical and horizontal directions respectively. For the rotor stations the vibration equations can be derived by the lumped parameters method or the finite element method (FEM); which is simple, hence neglected here. Now, we pay more attention to the modelling of the subsystem of gear coupling half, which includes a hub, a sleeve, and two sections j and $j+1$.

3.1. THE KINETIC ENERGY OF THE SUBSYSTEM

Let ε, δ denote the angles of a disc around axes ξ and η respectively. Hence, in the rotating co-ordinate system shown in Figure 2(b), the kinetic energy of the hub or sleeve can be written as

$$T_{jk} = \tfrac{1}{2} m\mathbf{V}_c \cdot \mathbf{V}_c + \tfrac{1}{2}\mathbf{G}\cdot\boldsymbol{\omega}, \quad k = e, i, \tag{19}$$

where

$$\mathbf{V}_c \cdot \mathbf{V}_c = \dot{x}^2 + \dot{y}^2 = \dot{\xi}^2 + \dot{\eta}^2 + \Omega^2(\xi^2 + \eta^2) + 2\Omega(\dot{\eta}\xi - \dot{\xi}\eta),$$

$$\mathbf{G}\cdot\boldsymbol{\omega} = J^d(-\dot{\varepsilon}\cos\delta - \Omega\cos\varepsilon\sin\delta)^2 + J^d(\dot{\delta} - \Omega\sin\varepsilon)^2$$

$$+ J^z[-\dot{\varepsilon}\sin\delta + (\Omega + \dot{\theta})\cos\varepsilon\cos\delta]^2.$$

The kinetic energy T of the subsystem is given by

$$T = T_{je} + T_{ji}, \tag{20}$$

where the subscripts je and ji denote the hub and sleeve of the gear coupling at station j.

3.2. THE POTENTIAL ENERGY OF THE SUBSYSTEM

The potential energy function U of the subsystem consists of two parts, one part is from the elastic deformation of the rotor sections beside the coupling, another part from the teeth

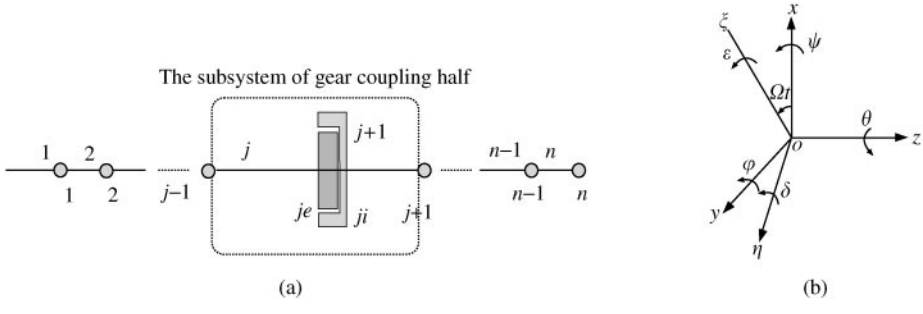

Figure 2. Rotor-gear coupling system and Co-ordinate systems.

deformation of the coupling that was modelled by Marmol [3] with the lateral and angular stiffness coefficients of the coupling.

$$U = U_s + U_c, \tag{21}$$

where

$$\begin{aligned}
U_s = {} & \frac{1}{2}\left(\frac{12EI}{l^3}\right)_j (\xi_{je} - \xi_{j-1})^2 - \left(\frac{6EI}{l^2}\right)_j (\xi_{je} - x_{j-1})(\delta_{je} + \delta_{j-1}) \\
& + \frac{1}{2}\left(\frac{4EI}{l}\right)_j (\delta_{je}^2 + \delta_{je}\delta_{j-1} + \delta_{j-1}^2) \\
& + \frac{1}{2}\left(\frac{12EI}{l^3}\right)_j (\eta_{je} - \eta_{j-1})^2 - \left(\frac{6EI}{l^2}\right)_j (\eta_{je} - \eta_{j-1})(\varepsilon_{je} + \varepsilon_{j-1}) \\
& + \frac{1}{2}\left(\frac{4EI}{l}\right)_j (\varepsilon_{je}^2 + \varepsilon_{je}\varepsilon_{j-1} + \varepsilon_{j-1}^2) \\
& + \frac{1}{2}\left(\frac{12EI}{l^3}\right)_{j+1} (\xi_{j+1} - \xi_{ji})^2 - \left(\frac{6EI}{l^2}\right)_{j+1} (\xi_{j+1} - \xi_{ji})(\delta_{j+1} + \delta_{ji}) \\
& + \frac{1}{2}\left(\frac{4EI}{l}\right)_{j+1} (\delta_{j+1}^2 + \delta_{j+1}\delta_{ji} + \delta_{ji}^2) \\
& + \frac{1}{2}\left(\frac{12EI}{l^3}\right)_{j+1} (\eta_{j+1} - \eta_{ji})^2 - \left(\frac{6EI}{l^2}\right)_{j+1} (\eta_{j+1} - \eta_{ji})(\varepsilon_{j+1} + \varepsilon_{ji}) \\
& + \frac{1}{2}\left(\frac{4EI}{l}\right)_{j+1} (\varepsilon_{j+1}^2 + \varepsilon_{j+1}\varepsilon_{ji} + \varepsilon_{ji}^2) \\
& + \frac{1}{2}\left(\frac{GI_p}{l}\right)_l (\theta_{je} - \theta_{j-1})^2 + \frac{1}{2}\left(\frac{GI_p}{l}\right)_{j+1} (\theta_{j+1} - \theta_{ji})^2
\end{aligned}$$

and

$$U_c = \frac{1}{2}k_l[(\xi_{ji} - \xi_{je})^2 + (\eta_{ji} - \eta_{je})^2] + \frac{1}{2}k_a[(\delta_{ji} - \delta_{je})^2 + (\varepsilon_{ji} - \varepsilon_{je})^2] + \frac{1}{2}k_t(\theta_{ji} - \theta_{je})^2.$$

3.3. THE DISSIPATION FUNCTION OF THE SUBSYSTEM

In terms of Marmol [3] the energy dissipation of the subsystem is from the internal damping of the coupling, which is a source of instability vibration. Then Rayleigh dissipation function $\tilde{R}$ in the rotating co-ordinate system can be expressed as

$$\tilde{R} = \frac{1}{2}c_l[(\dot{\xi}_{ji} - \dot{\xi}_{je})^2 + (\dot{\eta}_{ji} - \dot{\eta}_{je})^2] + \frac{1}{2}c_a[(\dot{\delta}_{ji} - \dot{\delta}_{je})^2 + (\dot{\varepsilon}_{ji} - \dot{\varepsilon}_{je})^2], \tag{22}$$

where the torsional damping is very small, hence neglected.

3.4. THE EQUATION OF MOTION

In theoretical analysis, although some condition such as large stiffness of the teeth is needed for equation (18), in a real turbo-machinery system it is easily satisfied. For example, the stiffness k_l is larger than 10^{10} N/m for gear coupling Type CL5. Thus, substituting equation (18) into expressions (20) and (21), then employing Lagrange's equation of motion

$$\frac{\mathrm{d}}{\mathrm{d}t}\left(\frac{\partial T}{\partial \dot{q}}\right) - \frac{\partial T}{\partial q} + \frac{\partial U}{\partial q} = -\frac{\partial \tilde{R}}{\partial \dot{q}}. \tag{23}$$

Here the generalized co-ordinates $q = \xi_{je}, \eta_{je}, \delta_{je}, \varepsilon_{je}, \theta_{je}, \xi_{ji}, \eta_{ji}, \delta_{ji}, \varepsilon_{ji}$.

Neglecting the higher orders, we can write the differential equations in the hub as

$$\begin{bmatrix} m_{je} + \frac{J_{ji}^z}{r_b^2}\cos^2\beta & \frac{J_{ji}^z}{r_b^2}\cos\beta\sin\beta & 0 & 0 & -\frac{J_{ji}^z}{r_b}\cos\beta \\ \frac{J_{ji}^z}{r_b^2}\cos\beta\sin\beta & m_{je} + \frac{J_{ji}^z}{r_b^2}\sin^2\beta & 0 & 0 & -\frac{J_{ji}^z}{r_b}\sin\beta \\ 0 & 0 & J_{je}^d & 0 & 0 \\ 0 & 0 & 0 & J_{je}^d & 0 \\ -\frac{J_{ji}^z}{r_b}\cos\beta & -\frac{J_{ji}^z}{r_b}\sin\beta & 0 & 0 & J_{je}^z + J_{ji}^z \end{bmatrix} \begin{Bmatrix} \ddot{\xi}_{je} \\ \ddot{\eta}_{je} \\ \ddot{\delta}_{je} \\ \ddot{\varepsilon}_{je} \\ \ddot{\theta}_{je} \end{Bmatrix}$$

$$- \begin{bmatrix} \frac{J_{ji}^z}{r_b^2}\cos^2\beta & \frac{J_{ji}^z}{r_b^2}\cos\beta\sin\beta & 0 & 0 & 0 \\ \frac{J_{ji}^z}{r_b^2}\cos\beta\sin\beta & \frac{J_{ji}^z}{r_b^2}\sin^2\beta & 0 & 0 & 0 \\ 0 & 0 & 0 & 0 & 0 \\ 0 & 0 & 0 & 0 & 0 \\ -\frac{J_{ji}^z}{r_b}\cos\beta & -\frac{J_{ji}^z}{r_b}\sin\beta & 0 & 0 & 0 \end{bmatrix} \begin{Bmatrix} \ddot{\xi}_{ji} \\ \ddot{\eta}_{ji} \\ \ddot{\delta}_{ji} \\ \ddot{\varepsilon}_{ji} \\ \ddot{\theta}_{ji} \end{Bmatrix}$$

$$- \begin{bmatrix} 0 & 2m_{je}\Omega & 0 & 0 & 0 \\ -2m_{je}\Omega & 0 & 0 & 0 & 0 \\ 0 & 0 & 0 & (2J_{je}^d - J_{je}^z)\Omega & 0 \\ 0 & 0 & -(2J_{je}^d - J_{je}^z)\Omega & 0 & 0 \\ 0 & 0 & 0 & 0 & 0 \end{bmatrix} \begin{Bmatrix} \dot{\xi}_{je} \\ \dot{\eta}_{je} \\ \dot{\delta}_{je} \\ \dot{\varepsilon}_{je} \\ \dot{\theta}_{je} \end{Bmatrix}$$

$$+\begin{bmatrix} c_l & & & & \\ & c_l & & & \\ & & c_a & & \\ & & & c_a & \\ & & & & 0 \end{bmatrix} \begin{Bmatrix} \dot{\xi}_{je} - \dot{\xi}_{ji} \\ \dot{\eta}_{je} - \dot{\eta}_{ji} \\ \dot{\delta}_{je} - \dot{\delta}_{ji} \\ \dot{\varepsilon}_{je} - \dot{\varepsilon}_{ji} \\ \dot{\theta}_{je} - \dot{\theta}_{ji} \end{Bmatrix}$$

$$-\begin{bmatrix} m_{je}\Omega^2 & & & & & \\ & m_{je}\Omega^2 & & & & \\ & & (J^d_{je} - J^z_{je})\Omega^2 & & & \\ & & & (J^d_{je} - J^z_{je})\Omega^2 & & \\ & & & & 0 \end{bmatrix} \begin{Bmatrix} \xi_{je} \\ \eta_{je} \\ \delta_{je} \\ \varepsilon_{je} \\ \theta_{je} \end{Bmatrix}$$

$$+\begin{bmatrix} \frac{12EI}{l^3} & 0 & -\frac{6EI}{l^2} & 0 & 0 \\ 0 & \frac{12EI}{l^3} & 0 & -\frac{6EI}{l^2} & 0 \\ -\frac{6EI}{l^2} & 0 & \frac{4EI}{l} & 0 & 0 \\ 0 & -\frac{6EI}{l^2} & 0 & \frac{4EI}{l} & 0 \\ 0 & 0 & 0 & 0 & \frac{GI_p}{l} \end{bmatrix}_j \begin{Bmatrix} \xi_{je} \\ \eta_{je} \\ \delta_{je} \\ \varepsilon_{je} \\ \theta_{je} \end{Bmatrix}$$

$$-\begin{bmatrix} \frac{12EI}{l^3} & 0 & \frac{6EI}{l^2} & 0 & 0 \\ 0 & \frac{12EI}{l^3} & 0 & \frac{6EI}{l^2} & 0 \\ -\frac{6EI}{l^2} & 0 & -\frac{2EI}{l} & 0 & 0 \\ 0 & -\frac{6EI}{l^2} & 0 & -\frac{2EI}{l} & 0 \\ 0 & 0 & 0 & 0 & \frac{GI_p}{l} \end{bmatrix}_j \begin{Bmatrix} \xi_{j-1} \\ \eta_{j-1} \\ \delta_{j-1} \\ \varepsilon_{j-1} \\ \theta_{j-1} \end{Bmatrix}$$

$$+\begin{bmatrix} k_l & & & & \\ & k_l & & & \\ & & k_a & & \\ & & & k_a & \\ & & & & 0 \end{bmatrix} \begin{Bmatrix} \xi_{je} - \xi_{ji} \\ \eta_{je} - \eta_{ji} \\ \delta_{je} - \delta_{ji} \\ \varepsilon_{je} - \varepsilon_{ji} \\ \theta_{je} - \theta_{ji} \end{Bmatrix}$$

$$+\begin{bmatrix} \frac{1}{r_b^2}\left(\frac{GI_p}{l}\right)_{j+1}+\frac{k_l}{r_b^2} & 0 & 0 & 0 & -\frac{1}{r_b}\left(\frac{GI_p}{l}\right)_{j+1}\cos\beta \\ 0 & \frac{1}{r_b^2}\left(\frac{GI_p}{l}\right)_{j+1}+\frac{k_l}{r_b^2} & 0 & 0 & -\frac{1}{r_b}\left(\frac{GI_p}{l}\right)_{j+1}\sin\beta \\ 0 & 0 & 0 & 0 & 0 \\ 0 & 0 & 0 & 0 & 0 \\ -\frac{1}{r_b}\left(\frac{GI_p}{l}\right)_{j+1}\cos\beta & -\frac{1}{r_b}\left(\frac{GI_p}{l}\right)_{j+1}\sin\beta & 0 & 0 & \left(\frac{GI_p}{l}\right)_{j+1} \end{bmatrix} \begin{Bmatrix} \xi_{je} \\ \eta_{je} \\ \delta_{je} \\ \varepsilon_{je} \\ \theta_{je} \end{Bmatrix}$$

$$+\begin{bmatrix} \frac{1}{r_b^2}\left(\frac{GI_p}{l}\right)_{j+1}+\frac{k_l}{r_b^2} & 0 & 0 & 0 & -\frac{1}{r_b}\left(\frac{GI_p}{l}\right)_{j+1}\cos\beta \\ 0 & \frac{1}{r_b^2}\left(\frac{GI_p}{l}\right)_{j+1}+\frac{k_l}{r_b^2} & 0 & 0 & -\frac{1}{r_b}\left(\frac{GI_p}{l}\right)_{j+1}\sin\beta \\ 0 & 0 & 0 & 0 & 0 \\ 0 & 0 & 0 & 0 & 0 \\ -\frac{1}{r_b}\left(\frac{GI_p}{l}\right)_{j+1}\cos\beta & -\frac{1}{r_b}\left(\frac{GI_p}{l}\right)_{j+1}\sin\beta & 0 & 0 & \left(\frac{GI_p}{l}\right)_{j+1} \end{bmatrix} \begin{Bmatrix} \xi_{ji} \\ \eta_{ji} \\ \delta_{ji} \\ \varepsilon_{ji} \\ \theta_{j+1} \end{Bmatrix}$$

$$= 0, \tag{24}$$

where

$$\sin\beta = \frac{\eta_{ji}-\eta_{je}}{\sqrt{(\xi_{ji}-\xi_{je})^2+(\eta_{ji}+\eta_{je})^2}}, \quad \cos\beta = \frac{\xi_{ji}-\xi_{je}}{\sqrt{(\xi_{ji}-\xi_{je})^2-(\eta_{ji}-\eta_{je})^2}}.$$

Since the equations in the sleeve have the same forms, we ignore then here.

Traditionally, the vibration models of the rotor system with a gear coupling we considered were divided into two uncoupled directions [3, 5, 7–9], or their generalized co-ordinates (or generalized displacements) are uncoupled both in the lateral and torsional directions; therefore, their dynamic characteristics are not affected by each other. However, from equation (24) we can see clearly that the inertia terms and elastic terms are coupled both in the lateral direction and torsional directions, respectively, and cannot be divided again. Meanwhile the system becomes non-linear at the station of gear coupling.

Assembling all the equations of motion of the stations, we can obtain the dynamic equations of the system [Figure 2(a)].

If some journal bearings existed in the rotors, the linearized stiffness and damping coefficients of oil film may be introduced as follows:

$$\begin{Bmatrix} \Delta F_x \\ \Delta F_y \end{Bmatrix} = \begin{bmatrix} k_{xx} & k_{xy} \\ k_{yx} & k_{yy} \end{bmatrix} \begin{Bmatrix} x \\ y \end{Bmatrix} + \begin{bmatrix} d_{xx} & d_{xy} \\ d_{yx} & d_{yy} \end{bmatrix} \begin{Bmatrix} \dot{x} \\ \dot{y} \end{Bmatrix}. \tag{25}$$

After transforming expression (25) into the rotating co-ordinate system, it becomes

$$\begin{Bmatrix} \Delta F_\xi \\ \Delta F_\eta \end{Bmatrix} = \begin{bmatrix} \cos \Omega t & \sin \Omega t \\ -\sin \Omega t & \cos \Omega t \end{bmatrix} \begin{Bmatrix} \Delta F_x \\ \Delta F_y \end{Bmatrix}. \tag{26}$$

Therefore equations of motion of the rotor-bearing-gear coupling system can be expressed as

$$[M]\{\ddot{\zeta}\} + [C]\{\dot{\zeta}\} + [K]\{\zeta\} = 0, \tag{27}$$

where the elements of the matrices $[M]$, $[C]$, and $[K]$ are not constant, they are functions of the generalized co-ordinates.

4. MISALIGNMENT AND NUMERICAL ANALYSIS

Figure 3 shows a simple configuration of the rotor-bearing-gear coupling system, at stations 4 and 5 where there are two gear coupling halves; according to equation (18) the constraint equations of the system are expressed as

$$\begin{aligned} r_b^2(\theta_{4i} - \theta_{4e})^2 &= (\xi_{4i} - \xi_{4e})^2 + (\eta_{4i} - \eta_{4e})^2, \\ r_b^2(\theta_{5i} - \theta_{5e})^2 &= (\xi_{5i} - \xi_{5e})^2 + (\eta_{5i} - \eta_{5e})^2. \end{aligned} \tag{28}$$

Therefore, there are totally 48 d.o.f. for the system.

Misalignment is unavoidable in the multirotor system. Two major kinds of misalignment for the gear couplings are the parallel and the angular shown in Figure 4(a) and (b) respectively.

4.1. PARALLEL MISALIGNMENT

Let a denote the initial parallel misalignment that coincides with the x-axis (the vertical direction) at station 4, then a translation is needed in the fixed co-ordinate system:

$$\begin{aligned} x_{4i} &= x_{4I} + a, \\ y_{4i} &= y_{4I}. \end{aligned} \tag{29}$$

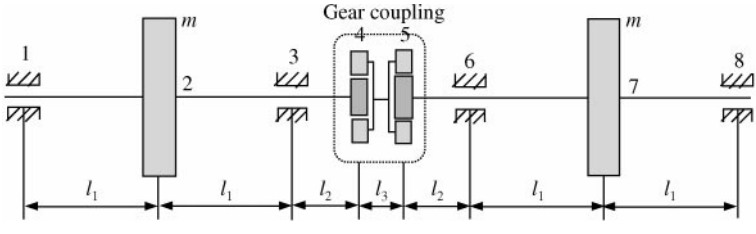

Figure 3. Rotor-bearing-gear coupling system.

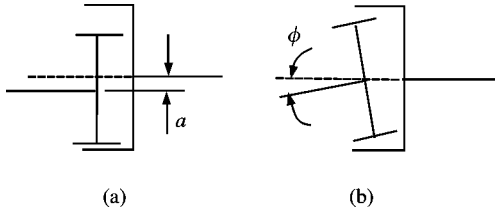

Figure 4. Misalignment of gear coupling: (a) parallel misalignment; (b) angular misalignment.

The two co-ordinate systems transformation between the rotating and the fixed [see Figure 2(b)] is written as

$$\begin{Bmatrix} \xi \\ \eta \end{Bmatrix}_{4j} = \begin{bmatrix} \cos \Omega t & \sin \Omega t \\ -\sin \Omega t & \cos \Omega t \end{bmatrix} \begin{Bmatrix} x \\ y \end{Bmatrix}_{4j}, \quad j = i, I. \tag{30}$$

Then

$$\begin{Bmatrix} \xi \\ \eta \end{Bmatrix}_{4i} = \begin{Bmatrix} \xi \\ \eta \end{Bmatrix}_{4I} + \begin{Bmatrix} a \cos \Omega t \\ -a \sin \Omega t \end{Bmatrix}. \tag{31}$$

4.2. ANGULAR MISALIGNMENT

Let ϕ denote the initial angular misalignment that rotated around the y-axis (the horizontal direction) at station 4, then in the fixed co-ordinate system the translation is

$$\begin{aligned} \varphi_{4i} &= \varphi_{4I} + \phi, \\ \psi_{4i} &= \psi_{4I}. \end{aligned} \tag{32}$$

Between the two co-ordinate systems shown in Figure 2(b), the transformation becomes

$$\begin{Bmatrix} \delta \\ \varepsilon \end{Bmatrix}_{4j} = \begin{bmatrix} \cos \Omega t & \sin \Omega t \\ -\sin \Omega t & \cos \Omega t \end{bmatrix} \begin{Bmatrix} \varphi \\ \psi \end{Bmatrix}_{4j}, \quad j = i, I. \tag{33}$$

Expression (33) may then be written as

$$\begin{Bmatrix} \delta \\ \varepsilon \end{Bmatrix}_{4i} = \begin{Bmatrix} \delta \\ \varepsilon \end{Bmatrix}_{4I} + \begin{Bmatrix} \varphi \cos \Omega t \\ -\phi \sin \Omega t \end{Bmatrix}. \tag{34}$$

For the right half (at station 5) the procedure is same.

Substituting equations (31), (34), into equation (27), it reads as

$$[M]\{\ddot{\zeta}\} + [C]\{\dot{\zeta}\} + [K]\{\zeta\} = \{F\}, \tag{35}$$

where the right-hand side matrix $\{F\} = \{\cdots \quad F_{4e}^{\mathrm{T}} \; F_{4i}^{\mathrm{T}} \; F_{5i}^{\mathrm{T}} \quad F_{5e}^{\mathrm{T}} \quad \cdots\}^{\mathrm{T}}$, in which

$$\{F_{4e}\} = \begin{Bmatrix} -\dfrac{J_i^z}{r_b^2} a\Omega^2 \cos(\Omega t + \beta_a)\cos\beta_a - c_l a\Omega \sin\Omega t \\ -\dfrac{J_i^z}{r_b^2} a\Omega^2 \cos(\Omega t + \beta_a)\sin\beta_a - c_l a\Omega \cos\Omega t \\ -c_a \phi\Omega \sin\Omega t \\ -c_a \phi\Omega \cos\Omega t \\ \dfrac{J_i^z}{r_b} a\Omega^2 \cos(\Omega t + \beta_a) \end{Bmatrix}, \tag{36}$$

$$\{F_{4l}\} = \begin{Bmatrix} \dfrac{J_i^z}{r_b^2} a\Omega^2 \cos(\Omega t + \beta_a)\cos\beta_a + c_l a\Omega \sin\Omega t \\ \dfrac{J_i^z}{r_b^2} a\Omega^2 \cos(\Omega t + \beta_a)\sin\beta_a + c_l a\Omega \cos\Omega t \\ c_a \phi\Omega \sin\Omega t \\ c_a \phi\Omega \cos\Omega t \\ 0 \end{Bmatrix}, \tag{37}$$

and

$$\beta_a = \tan^{-1} \frac{\eta_{4l} - \eta_{4e} - a\sin\Omega t}{\xi_{4l} - \xi_{4e} + a\cos\Omega t}.$$

The matrices $\{F_{5i}\}$, $\{F_{5e}\}$ are of the same form as $\{F_{4i}\}$, $\{F_{4e}\}$.

Equation (35) is the motion equation of the coupled lateral torsional vibration of the system with misaligned gear coupling, and is a set of non-linear differential equations which are periodic functions of time in the rotating co-ordinate system. In expressions (36) and (37), we can find that the forces due to the misalignment consist of two parts, one related to $J_i^z a\Omega^2/r_b^2$ is clearly from the inertia force of the sleeve of a gear coupling, and the other related to $c_l a\Omega$ is from the damping of the gear coupling; hence the amplitudes of the steady state vibration of the misaligned system are related to the misalignment, internal damping, the rotating speed, and the structural parameters of the gear coupling.

The inertia force of the sleeve due to misalignment is equal to $J_i^Z a\Omega^2/r_b^2$ that coincides with the x-axis. Based on Newton's laws it reacted on the teeth of the hub along the engagement line, and equals $F'_{gi} = J_i^Z a\Omega^2 \cos(\Omega t + \beta_a)/r_b^2$ shown in Figure 5. The force F'_{gi} can be equivalently replaced by a force and a moment. The former F_{gi} acts on the center O_e of the hub, and the later M_{gi} acts on the hub in the torsional direction. Furthermore, the components of F_{gi} in x and y directions are

$$F_{gx} = -J_i^z a\Omega^2 \cos^2(\Omega t + \beta_a)/r_b^2 = -J_i^z a\Omega^2 [\cos(2\Omega t + 2\beta_a) + 1]/2r_b^2, \tag{38}$$

$$F_{gy} = -J_i^z a\Omega^2 \cos^2(\Omega t + \beta_a)\sin(\Omega t + \beta_a)/r_b^2 = -J_i^z a\Omega^2 \sin(2\Omega t + 2\beta_a)/2r_b^2 \tag{39}$$

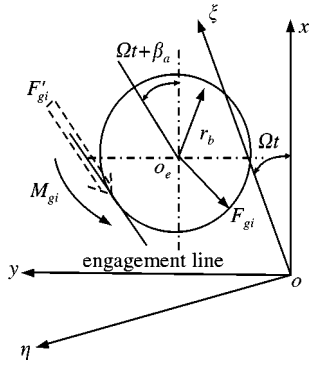

Figure 5. The inertia force and moment acted on the hub.

and the moment is

$$M_{gi} = J_j^z a\Omega^2 \cos(\Omega t + \beta_a)/r_b. \tag{40}$$

From equations (38)–(40), we can find by supposing β_a equal to constant, that equation (35) is linear, and the force components in x and y directions in its right terms become periodic functions of time in two integer multiple rotating speed. Then based on the theory of linear vibration the response in lateral (x and y) direction is of two integer multiple components of the rotating speed, and from equation (40) for the same reason the response in the torsional direction has the component of the rotating speed. In general β_a is not a constant, and is a function of time and the generalized co-ordinates. Thus, equation (35) is non-linear. Its dynamic analysis in theory is difficult for the system, therefore, numerical analysis is required.

Using the same method we can investigate the force from $c_l a\Omega$. The integer multiple components will also occur in the response.

In the past works, the response or vibration signature of the rotor -bearing system with a misaligned gear coupling in the lateral direction was considered more, and that in the torsional direction was ignored. In the above modelling and analysis we know that the responses in the two directions are related to each other because of the coupled vibration. This dynamic behavior is very important in the fault diagnosis analysis of the misaligned system.

4.3. RESULTS OF NUMERICAL INTEGRATION

To study the signature of the rotor-bearing-gear coupling system show in Figure 3, an analysis using numerical integration has been performed for two uniform symmetrical rotors supported at the ends in journal bearings connected by a gear coupling Type CL5.

Consider the values of the system: rotors $l_1 = 0{\cdot}5$ m, $l_2 = 0{\cdot}15$ m, $d = 0{\cdot}09$ m, $\Omega = 314{\cdot}16$ rad/s, $E = 206$ GPa, $G = 80$ GPa, $m = 700$ kg, $J^z = 12{\cdot}0$ kg m^2, $J^d = 6{\cdot}0$ kg m^2; bearings (at stations 1 and 8) $k_{xx} = 1{\cdot}274 \times 10^8$ N/m, $k_{xy} = -0{\cdot}215 \times 10^8$ N/m, $k_{yx} = 1{\cdot}520 \times 10^8$ N/m, $k_{yy} = 0{\cdot}812 \times 10^8$ N/m, $c_{xx} = 7{\cdot}906 \times 10^5$ N s/m, $c_{xy} = 2{\cdot}633 \times 10^5$ N s/m, $c_{yx} = 2{\cdot}633 \times 10^5$ N s/m, $c_{yy} = 3{\cdot}143 \times 10^5$ N s/m, bearings (at stations 3 and 6) $k_{xx} = 1{\cdot}477 \times 10^8$ N/m, $k_{xy} = -0{\cdot}197 \times 10^8$ N/m, $k_{yx} = 1{\cdot}683 \times 10^8$ N/m, $k_{yy} = 0{\cdot}882 \times 10^8$ N/m, $c_{xx} = 8{\cdot}698 \times 10^5$ N s/m, $c_{xy} = 2{\cdot}865 \times 10^5$ N s/m, $c_{yx} = 2{\cdot}865 \times 10^5$ N s/m,

$c_{yy} = 3{\cdot}268 \times 10^5$ N s/m; gear coupling, $k_l = 1{\cdot}8 \times 10^{10}$ N/m, $k_a = 0{\cdot}0$ N/m, $k_t = 8{\cdot}04 \times 10^6$ N m/rad, $c_l = 1{\cdot}10 \times 10^6$ N s/m, $c_a = 86{\cdot}2$ N m s/rad, $r_b = 0{\cdot}0798$ m^2, $\alpha = 20^\circ$, $l_3 = 0{\cdot}15$ m, $a = 0{\cdot}20 \times 10^{-3}$ m, $\phi = 0{\cdot}44 \times 10^{-2}$ rad.

Figure 6 shows the steady state response diagrams and their frequency spectra at running speed, it may be seen that the even-integer multiples of the rotating speed of lateral vibration and the odd-integer multiples of the torsional vibration occurred in the

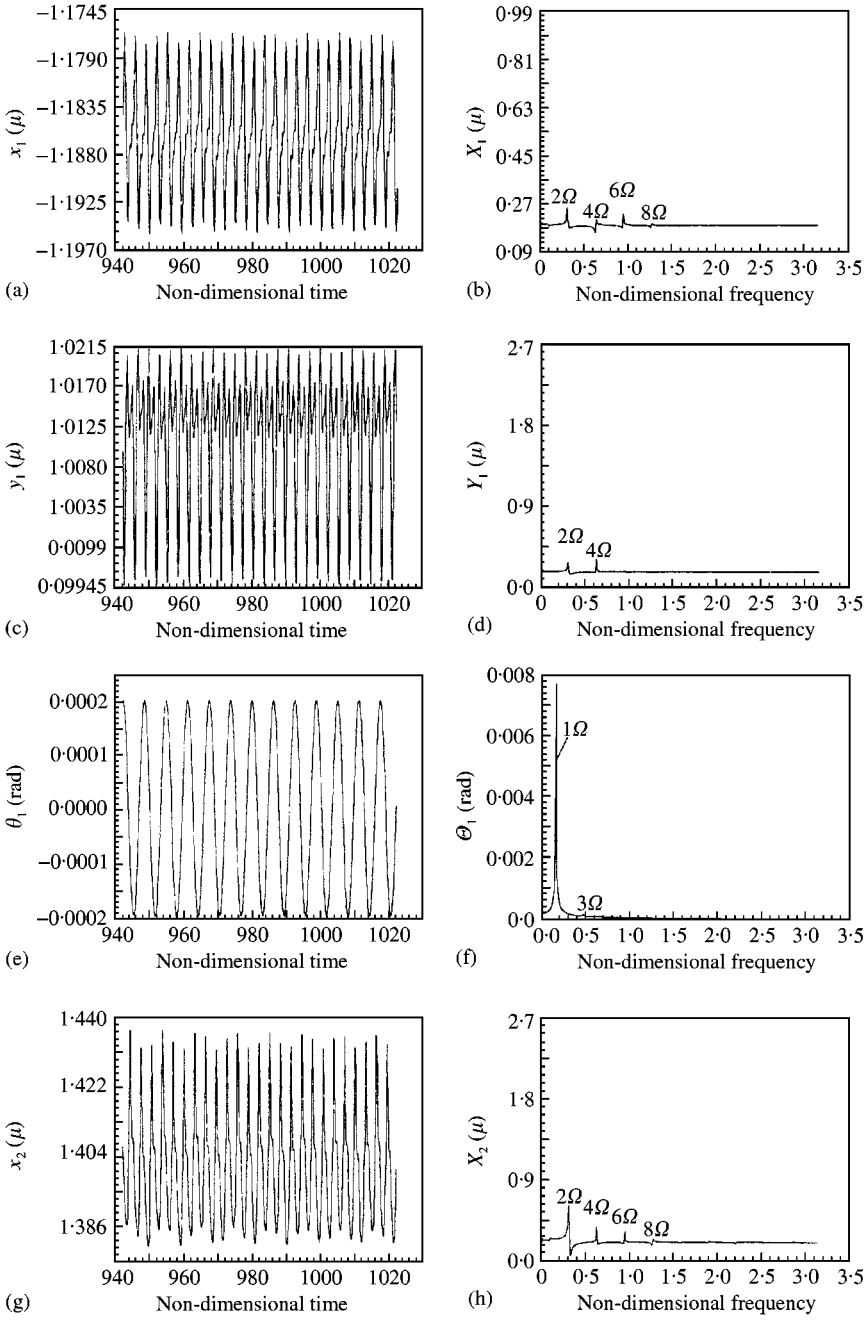

Figure 6. Steady state responses of the system and their frequency spectrums at running speed.

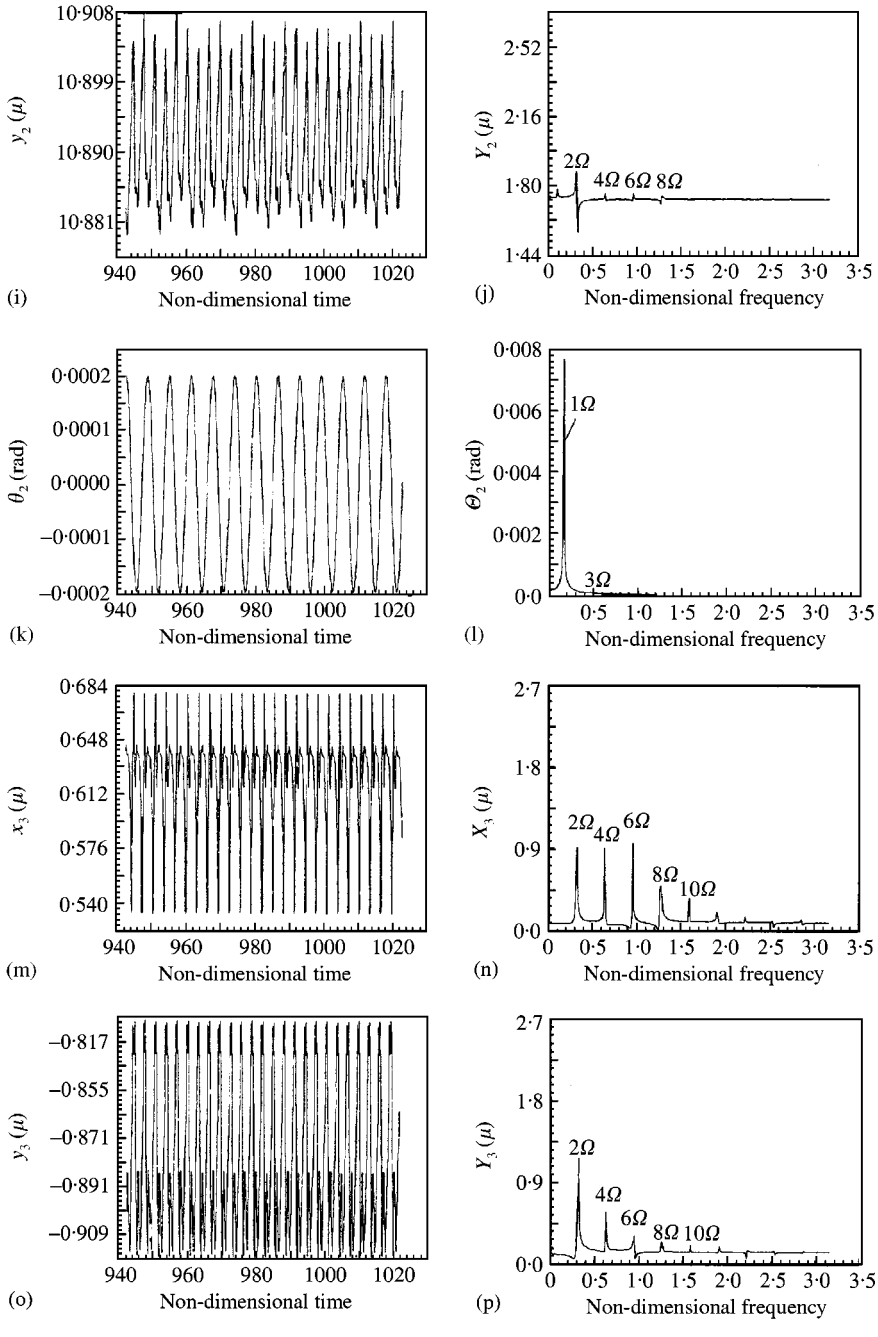

Figure 6. Continued.

misaligned system, and the integer multiples of vibration are apparent around the gear coupling. The vibrations of rotors far away from the coupling are not visible. Therefore, those would provide more detailed information for the fault diagnosis of the gear coupling misalignment in the multirotor system. After calculating, it is found that the responses increase with an increase in the misalignment as well as the damping coefficients of gear couplings.

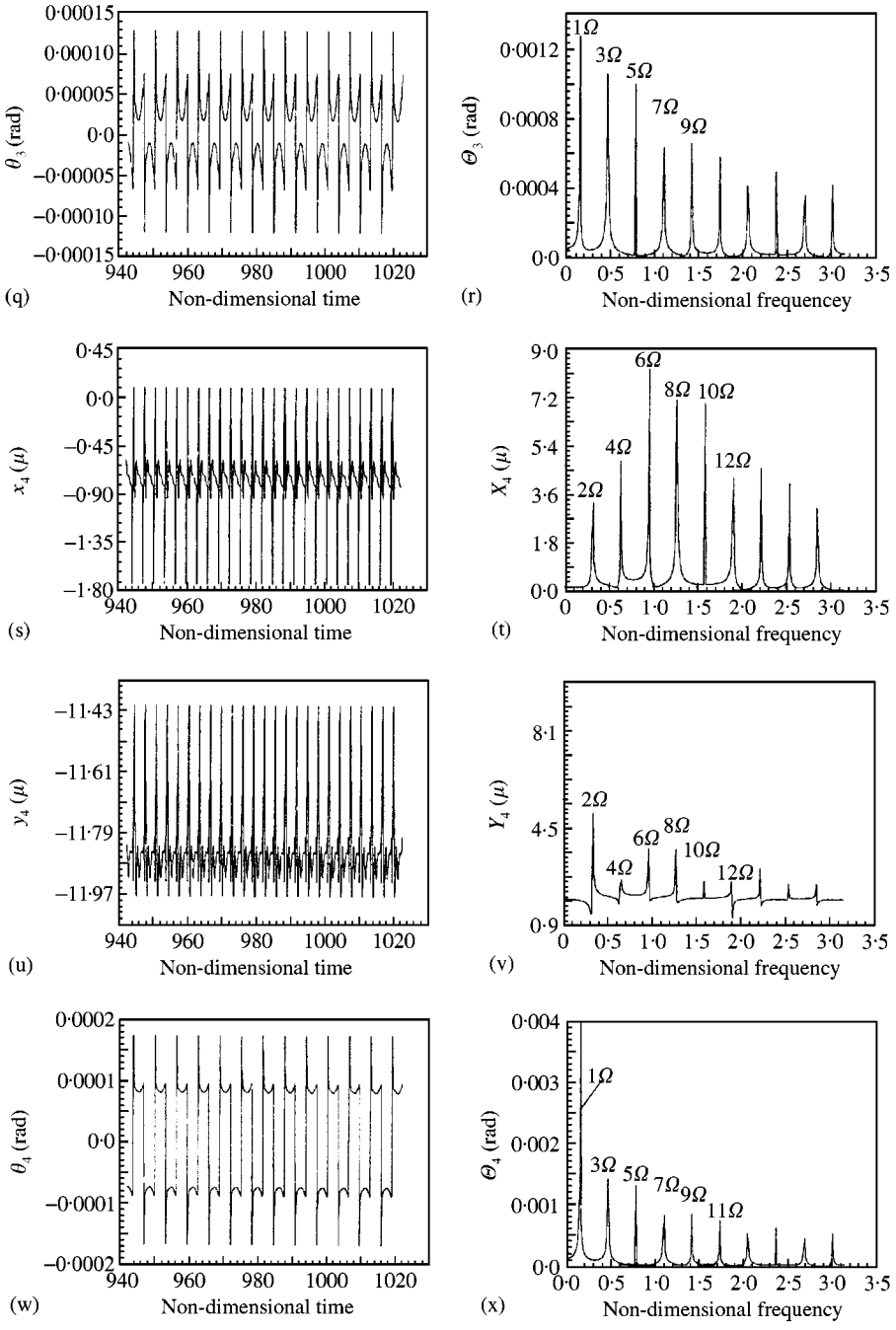

Figure 6. Continued.

Traditionally, the damping (or internal friction) of gear coupling was considered because it can cause instability to the system. From the above analysis, we can find that the damping not only affects the stability of the system, but also causes the vibration of integer multiples components. In general, the damping of the system is mainly from the journal bearings (oil

film force), that from the gear coupling is not large, hence it decreases the stability threshold speed little. But the damping from gear couplings can cause the integer multiples vibration both in the lateral and torsional directions, which may create the harmonic resonance of the system and could cause the damage to the system.

5. CONCLUSIONS

Based on the engagement conditions of gear couplings, the holonomic constraint equation describing an inherent relationship between the lateral displacements in the centers and torsional angles of the mating gears is derived, which implies a coupling of the lateral and torsional d.o.f. and is the primary source due to the coupled vibrations between lateral and torsional directions in multirotor systems with a gear coupling. Thereby the vibrations in the two directions cannot be considered independently.

The non-linear coupled lateral torsional vibration model of a multirotor system with a gear coupling is developed from Lagrange's equation. Theoretical analysis shows that the forces and moments acting on gear couplings due to the initial misalignment are from the inertia forces of the sleeve and the internal damping between the meshing teeth. The amplitudes of the steady state vibration of the system are related to the misalignment, internal damping, the rotating speed, and the structural parameters of the gear coupling.

Numerical analysis for the signature of vibration reveals that the even-integer multiples of the rotating speed of lateral vibration and the odd-integer multiples of the torsional vibration occurred in the misaligned system, and the integer multiples of vibration are apparent around the gear coupling. The vibrations of rotors far away from the coupling are not visible.

ACKNOWLEDGMENT

The authors are grateful for the financial support from National Science Foundation of China (Grant No. 19990511).

REFERENCES

1. D. L. DEWELL and L. D. MITCHELL 1984 *Journal of Vibration, Acoustics, Stress and Relibility in Design* **106**, 9–16. Detection of a misaligned disk coupling using spectrum analysis.
2. C. B. GIBBONS 1976 *Proceedings of the 5th Turbo-machinery Symposium,* 111–116. Coupling misalignment forces.
3. R. A. MARMOL 1980 *Journal of Mechanical Design* **102**, 168–176. Spline coupling induced nonsynchronous rotor vibrations.
4. SHIGEO NAWATE and YOSHIO TERAUCHI 1995 *JSME International Journal* **38**, 106–111. Number of teeth in contact and load capacity of gear-type shaft coupling.
5. SHINGO YAMAUCHI and TSUNEO SOMEYA 1980 *Transactions of the Japan Society of Mechanical Engineers, Part C* **46**, 806–814. The study of a gear coupling (the non-linear vibration analysis of rotors which have one gear coupling).
6. M. M. CALISTRAT 1981 *Journal of Mechanical Design* **103**, 54–60. Fraction between high speed gear coupling teeth.
7. E. KRAMER 1993 *Dynamics of rotors and foundations.* Berlin: Springer-Verlag.
8. N. BACHSCHMID, A. CURAMI and F. PETRONE 1992 *Proceedings of the International Conference on Rotor Machine Dynamics*, 232–239. Vibrational behaviour of rotors with gear couplings in case of insufficient coupling lubrication.
9. YOICHI KANEMITSU 1985 *Bulletin of JSME* **28**, 3002–3009. Torsional vibration of rotor coupled by gear coupling.

10. C. P. R. KU, J. F. WALTON, J. W. LUND 1994 *Journal of Vibration and Acoustics* **116**, 250–256. Dynamic coefficients of axial spline couplings in high-speed rotating machinery.
11. M. XU and R. P. MARAGONI 1994 *Journal of Sound and Vibration* **176**, 663–679. Vibration analysis of a motor-flexible coupling-rotor system subject to misalignment and unbalance. Part I: Theoretical model and analysis.

APPENDIX A: NOMENCLATURE

a	parallel misalignment at station 4
c_l, c_a	lateral and angular damping coefficients of gear coupling respectively
c_{xx}, c_{xy}, c_{yx}, c_{yy}	damping coefficients of oil bearing film
d	diameter of rotor
E	Young's modulus
F	force
G	shear modulus
I	moment of inertia of section
J^d, J^z	diameter and polar moment respectively
k_l, k_a	lateral and angular stiffness coefficients of gear coupling respectively
k_t	torsional stiffness coefficients of gear coupling
k_{xx}, k_{xy}, k_{yx}, k_{yy}	stiffness coefficients of oil bearing film
l	length
m	mass
M	moment
r_b	radius of base circle of gear coupling
R	dissipation function
t	time
T	kinetic energy
U	potential energy
x, y	displacements of vertical and horizontal directions respectively
X, Y	amplitudes of frequency spectrum of x and y respectively
Ω	rotor speed
α	pressure angle of gear
β	angular
ϕ	angular misalignment at station 4
θ, Θ	torsional angle and its amplitude of frequency spectrum respectively
$[M]$, $[C]$, $[K]$, $[F]$	matrices defined by equations (19) and (27)

Subscripts

a, l, t	angular, lateral and torsional directions
e, i	hub and sleeve of gear coupling
i, j	ith and jth shaft section (or node)
x, y	x and y components in lateral direction

Superscripts

d, z	diameter and z (or polar) direction
$\cdot$, $\ddot{}$	derivative with time